CHAPTER-2

CHAPTER 2

LITERATURE REVIEW

This chapter critically assesses the available research on surface texturing and its significance in improving the friction and wear performance of bodies in relative motion. The chapter begins by highlighting the importance of surface interactions in governing the wear behaviour of mating bodies, which is followed by a brief introduction to friction and wear phenomena. A brief description of the different theories of friction and types of wear, along with the methods of minimising them, also forms a part of the chapter. Further, exhaustive literature regarding the texturing, properties, applications and methods of synthesis have been presented. Special attention has been given to the research being conducted in regard to the application of texturing, both in dry and lubricated conditions, in improving the friction and wear characteristics of a tribo-pair. In the end, the formulation of the problem for the current investigation has been included.

2.1 SURFACE INTERACTIONS AND WEAR

Surface interactions occur when two bodies come in physical contact with each other. Without physical contact, there is no friction, no wear or other contact phenomena. Surface interaction, therefore, is an important phenomenon in engineering contact problems and depends readily on the surface characteristics, contact type, surface material etc.

The surface is not simple. All the engineering surfaces have irregularities in the form of asperities, as shown in Fig. 2.1 (a). These irregularities, as gross surface geometric characteristics of solids, are inherent in the production process and termed roughness. The roughness is quantified by measuring variation in the direction of the normal vector of an actual

surface from its ideal form and the surface gets rough if these deviations are considerable. The surface with small deviations is considered smooth, usually has a lower coefficient of friction, and undergoes wear slowly than a rough surface. The statistical parameters R_a, CLA (centre-line average), or AA (arithmetic average) and the standard deviation or variance (σ), R_q or root mean square (RMS) are used in general to characterize surface roughness. Skewness (S_k) and kurtosis (K) are the other statistical parameters which are rarely used. R_t (maximum peak-to-valley height), R_p (maximum peak height), R_v (maximum valley depth), R_z (average peak-to-valley height), and R_{pm} (average peak-to-mean height) are the statistical parameters that are used to characterize the roughness when R_a, R_q are not sufficient to describe the functional characteristics. Surface roughness measurement can be done either by mechanical or optical methods. A surface roughness tester, atomic force microscope (AFM), profilometer, and scanning laser microscope are used for this purpose (Bhushan, 1999).

The irregularities or asperities on the solid surface itself are covered with various films. For example, as shown schematically in Fig. 2.1. (b), an environmental adsorbate such as water vapour or hydrocarbons may have condensed and been adsorbed physically to the solid surface on the outermost physisorbed layer. A chemisorbed layer may be present when adsorbed species form an electronic bond with the solid surface. It is limited to a monolayer through metal, or alloy oxide is generally present beneath the physisorbed layer on metallic surfaces or alloys. The layers of metals and many non-metals oxides, nitrides, sulphides and chloride are formed depending on the environment over the chemically reactive surfaces. For example, macroscopic phenomena, like corrosion, may occur in the presence of atmospheric oxygen. Fig. 2.1 (c) shows the interaction which is mainly brought about by the continuously changing contact topography with time and relative displacement. A work-hardened or deformed layer because of grinding or polishing is found, which is micro-crystalline in nature and termed as the Beilby layer (Beilby, 1921). The mechanical behaviour of the Beilby layer

depends on the amount of depth deformation of the layer. The next layer is the one which has been mechanically heavily deformed due to large accumulated residual stresses. Beneath the severely deformed region are layers of less deformed material. The depth of all the regions is mentioned in Fig. 2.1(b). The last layer is of undeformed material. The existence of surface films has an impact on friction and wear.

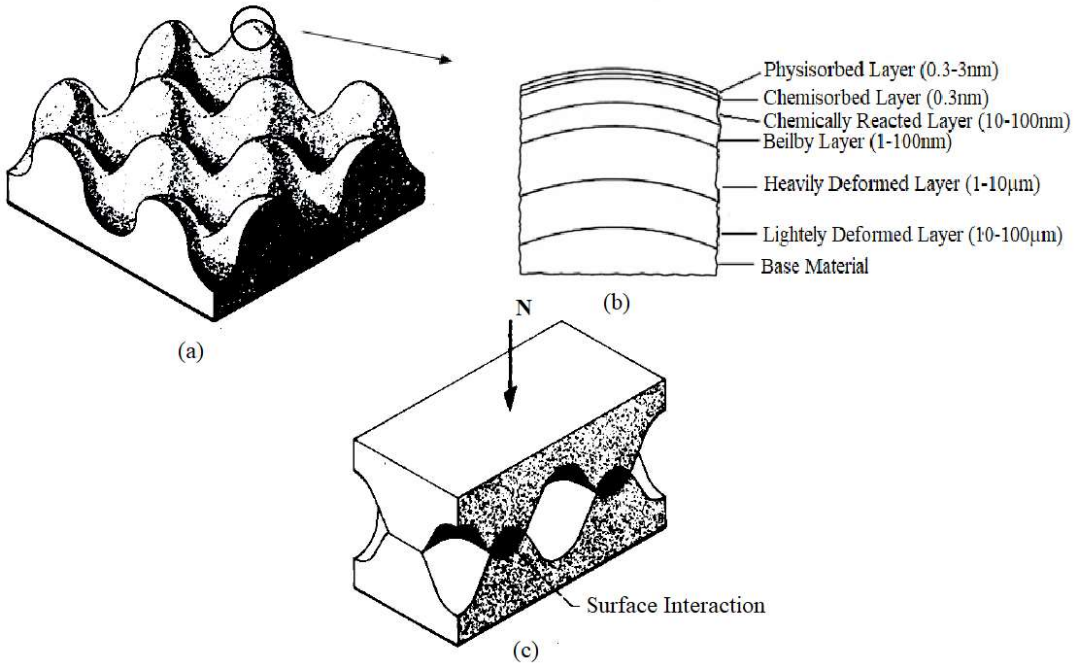

Fig. 2.1 Schematic diagram of surface topography, various surface films and interaction at asperities. (Buckley, 1981)

2.1.1 SURFACE CONTACTS

As seen in Fig. 2.1 (c), the actual contact between two solid surfaces occurs at the points of the asperities or surface imperfections. Because of this, the real area of contact is substantially smaller than the apparent area of contact (Archard, 1953). When the load is sufficiently high, the deformation at asperity areas is initially elastic and then deforms plastically until the load can be supported. With deformation, the real contact area increases

until it is large enough to support the imposed load. The real contact area is directly proportional to normal load when there is the plastic deformation of the asperity is plastic in a single asperity contact and is given by the equation,

$$A_r = \frac{N}{p} \text{ (Rabinowicz, 1965)}$$

where p is the mean yield stress of asperities of softer of the two materials in contact, and N is the applied load.

Bowden & Tabor (1950, 1964) demonstrated that during plastic deformation, the contact could be considered a small hardness indentation, and the mean contact pressure is independent of load, contact geometry and equal to the hardness. In this case, the real area of contact A_{rp} is, therefore, independent of the apparent area, inversely proportional to the hardness and proportional to the normal load.

Also, the surface layers generally deform with the deformation of the surfaces. Depending on their mechanical qualities, these surface layers may be compliant with the surface and deform with it, or they may get disrupted or dislodged. As a result, when the surface films break up, solid-state clean material contact occurs at the asperity junctions, and the basic material properties of the solids contribute to the materials' friction and wear behaviour.

2.1.2 FRICTION

The resistance to motion arising from the interaction between the contacting surfaces is known as friction. It is a reaction force due to system response, not a material property. Friction can be thought of tangential component of the contact force originating from mechanical engagement arising from surface roughness. However, in many cases, like the friction coefficient of the super-finished surface increases sharply instead of decreasing, a very thin polar molecular adsorption layer can significantly decrease the frictional force. The dry

friction, also called “Coulomb” friction, occurs between two solid surfaces. Fluid friction, which is typically investigated under lubrication, arises when adjacent layers in a fluid move at different speeds in relation to one another. The friction force is a resisting force but can be maximised or minimised depending on the application.

The two categories under which dry friction is classified are static friction (stiction) and kinetic friction (also termed sliding/ dynamic friction). Static friction is defined between stationary surfaces, whereas kinetic friction appears between sliding surfaces. The elementary property of dry friction is expressed as the following three empirical laws, two of which were given by Amontons (1699), and the third law was added by Coulomb (1785).

1. The force of friction is directly proportional to the applied load. (Amontons 1st Law)

2. The friction force is independent of the apparent contact area. (Amontons 2nd Law)

3. Kinetic friction is independent of the sliding velocity. (Coulomb's Law)

The expression for friction coefficient from Amontons 1st law can be calculated using ordinary mathematics:

$$F = \mu N$$

where F = friction force, N= normal force and μ is a constant of proportionality known as the coefficient of static friction (μ_s) or kinetic friction (μ_k) and is independent of the normal load. Coulomb proposed that metallic friction arises due to the mechanical interaction of wedge-shaped asperities of the contacting surfaces. Coulomb's model failed to address the dissipative nature of friction, and the mechanical interaction theory was exempted.

Bowden & Tabor (1950, 1964, 1973) proposed the adhesion theory, which was widely accepted. They suggested that two metals in sliding contact by applying a tangential force and, due to high pressures developed at individual contact spots, lead to interfacial adhesion between asperities and shearing to accommodate the relative motion. Friction is caused by two

forces: an adhesion force arising at the actual point of contact (asperity junctions) and a delamination force required to plough the asperities of the harder surface through the softer ones. The tangential force can be written in terms of the force needed to shear adhered junctions (F_a) and the force required to provide the energy for deformation (F_d)

$$F = F_a + F_d$$

The major force of friction is the force required to shear the junctions formed between the two bodies at the real area of contact. This force of friction is given by:

$$F_a = \tau_a A_r$$

where τ_a is the average shear strength of the dry contact, which is a function of the materials of the bodies (and of any intervening surface film). The coefficient of friction (μ_a) is then given by the following equation:

$$\mu_a = \frac{F_a}{N} = \frac{\tau_a A_r}{H A_r} = \frac{\tau_a}{H}$$

where H is the hardness of the softer of the contacting materials. The coefficient of friction μ is, therefore, expressed as

$$\mu = \frac{F_a + F_d}{N} = \mu_a + \mu_d$$

Where, N is the applied normal load on the contacting surface, μ_a and μ_d are the friction coefficients due to adhesion and deformation, respectively.

2.1.3 WEAR

Wear is characterised as an ongoing process of material degradation or loss from surfaces that come into contact with a relative movement. Wear is also a system response and

the inevitable result of friction. In applications like writing with a pencil, machining, polishing wear is desirable, whereas bearings, gears, seals and other machine applications are meant to minimize wear. (Bhushan, 1999)

Material removal from a solid surface can occur by either fracture, dissolving, or melting; however, all three can be observed in some types of wear. On this basis, wear can be categorized into abrasive or non-abrasive. (Stachowiak, 2005)

2.1.3.1 TYPES OF WEAR

The different types of wear can be classified based on the basic material removal mechanisms on a microscopic level and conditions. Two major categories of wear based on wear mechanisms and conditions are abrasive and non-abrasive types. The more descriptive expressions for wear are (i) abrasive wear, (ii) adhesive wear, (iii) erosive wear, (iv) impact wear, (v) fatigue wear (vi) corrosive wear. (Hutchings, 1992)

Abrasive wear occurs between a hard rough surface in sliding contact with a softer surface. The removal or displacement of softer material is caused by the harder asperities of another surface or loose particles. Hard particles remove material from the opposing surface, causing two-body abrasion. Three-body abrasion occurs when free-to-roll particles are present between the surfaces. The relative hardness significantly influences abrasive wear characteristics. The three most frequently recognised abrasive wear mechanisms are ploughing, cutting, and fragmentation. This type of wear causes high wear rates and extensive damage to the surface. **Adhesive wear** occurs when asperities on the opposing surfaces in sliding contact get fused and are then subsequently ruptured due to their relative motion. The load and surface temperature are the two most important external elements that influence adhesive wear. Due to material transfer between the two surfaces, adhesive wear can cause an increase in roughness and the formation of protrusions. This type of wear takes place commonly and is hard to be

eliminated. **Erosive wear** is a combination of impact and abrasive wear. In erosive wear, due to mechanical action from fluids or solid particles, progressive material removal processes occur and can be named solid erosion and fluid erosion accordingly. **Impact wear** is described as the removal of material and damage to a solid surface caused by repetitive impacts from another solid. Impacts cause subterranean cracks to propagate to the surface. The capacity of impact wear is related to impact energy. **Fatigue wear** refers to a process in which detachment of the wear particles occurs by cyclic growth of microcracks on the surface or subsurface region of a material that is weakened by cyclic loading. Surface fatigue wear is inevitable, and generally, pits are formed on the surface due to fatigue wear under the action of the cycle contact stress. **Corrosive wear** is the damage caused by a synergistic effect of corrosion at a surface and any of the mechanical wear mechanisms. The corrosive wear in the air is generally called oxidative wear. The sliding surfaces experience corrosive wear in a corrosive environment, and a rise in the sliding velocity accelerates the wear rate. However, in some cases, the direct metal-metal contact is prevented by reaction layers, such as oxide films formation, which act as a solid lubricant.

It has also been seen that the type of wear may change due to the variation in working conditions. For example, with the increase in sliding velocity under a fixed load, wear at the surface may change from oxidation wear to adhesive wear. (Halling, 1975)

2.2 MINIMISATION OF FRICTION AND WEAR

The dissipation of energy due to friction primarily manifests as heat and causes huge economic losses. Energy conservation through friction minimization and control of friction is a major concern. It is essential to look for efficient ways to utilise energy in particular applications (like automotive brakes and clutches) where high friction is necessary. Similarly, wear causes wastage of material, which is the next major concern. It reduces the component

lifetime leading to loss of mechanical performance, catastrophic failure and hence considerable cost involvement. Wear is generally not desired in most industrial applications. Friction and wear can be notably reduced by employing different techniques like lubrication and surface engineering.

A lubricant is a substance that helps to minimise friction and wear between surfaces in relative motion. It may be solid, liquid or gas. Lubrication is an old and widespread method to reduce friction as well as wear and allows smooth running of machine/ components. Surface engineering is another technique to minimise friction and wear, which involves altering the surface properties and hence optimizing its function during the interaction with the surrounding systems. Surface engineering techniques could be roughly classified between surface finishing and surface texturing. The surface finishing typically regards structural modifications by addition, removal, or chemical alteration of material. Whereas surface texturing involves topographical modifications through various manners of surface reshaping. The textures on the surface act as a storage pocket for liquid lubricant (in full fluid-film and mixed lubrication) or wear debris (in dry and boundary lubrication), which significantly improve tribological performance. The appropriate selection of texture parameters is needed to get the desired friction and wear output. (Grützmacher et al., 2019; Vencl et al., 2019) On the other hand, the coating is a layer of material deposited on the surface of the base material to enhance its tribological properties. The coating can be classified as hard (wear-resistant coatings) and soft (low-friction coatings) based on the nature of the coated surface. Microstructural treatment can also improve the surface hardness of the material, which causes an increased wear resistance. (Bhushan, 1999) Unlike other ways to control friction and wear, it is a relatively cheap way to improve tribological properties without applying any special material. The most common microstructural treatments are carburising, nitriding, flame hardening, laser hardening, electron beam hardening, work hardening, and shot peening.

2.3 LUBRICATION

The word lubricant has been derived from the Latin word 'lūbricāre', which means 'to make slippery'. A lubricant's principal role is to protect moving parts, decreasing friction and wear on the machine. Adding a lubricant to a solid-solid contact reduces friction, which means less wear, heat generation, and energy loss, lowering operational costs and downtime. Cooling and debris removal is desirable secondary benefits provided by a fluid lubricant. Based on the physical state, the lubricants may be classified as:

(i) **Liquid lubricants:** Mineral oil or synthetic oils, vegetable oils, animal oils.

(ii) **Semi-solid lubricants:** Greases and waxes.

(iii)**Solid lubricants:** Graphite, MoS_2, PTFE, hBN.

(iv)**Gaseous lubricants:** Atomized oils, Nitrogen, Helium.

Liquid lubricants provide a lubrication film between the friction surfaces, allowing a load to be carried with minimal shear stress, reducing friction and material degradation. The base oil and additives constitute the majority of liquid lubricants. Based on their origin, liquid lubricants can be classified as vegetable oil, animal oil, olive oil, mineral oil, synthetic lubricant etc. A good lubricant generally possesses the following properties: (i) adequate viscosity to maintain a lubricant film for particular service conditions, (ii) high boiling point, (iii) low freezing point, (iv) stable under oxidation and thermal stresses (or low volatility), (v) corrosion resistant.

Semi-solid lubricants are used in several applications where the lubricant must not run out or for higher temperature applications. Blending a lubricating oil base with thickening additives yields a semi-solid lubricant. Special soaps of Li, Na, Ca, etc., are the primary type of thickener, but there are other non-soap thickeners such as carbon black, silica gel, polyureas, and other synthetic polymers. The most common semi-solid lubricants are greases, usually

produced by emulsifying the oil with soap. At lower speeds, grease can handle a significantly larger load. Grease, on the other hand, has a far higher internal resistance than lubricating oils and is, therefore, more difficult to handle for dispensing, draining, and replenishing than oil.

Solid lubricants are recommended when operating conditions prevent lubricating oils or grease from securing a lubricating film. Solid lubricants are applied either in the form of a coating or as additives in liquid lubricants, greases and composites. Graphite, molybdenum disulphide, tungsten disulphide, and zinc oxide are widely used solid lubricants. They have high-temperature stability and load-carrying capacity.

Sir Isaac Newton's (1687) fundamental law of viscosity, which states that at every point in a fluid, the shearing stress is proportional to the rate of shear of the fluid subjected to a mechanical force, can be linked to the modern history of lubrication. Non-Newtonian fluids are materials that do not obey this law, such as ketchup. Amontons (1699) and Coulomb (1785) proved that the ratio is constant between tangential resistance and the normal component of the load for dry and imperfectly lubricated surfaces for a given range of contact area, speed, and load. In his research, Rennie (1829) concluded that the composition of the solid surfaces was primarily responsible for the degree of wear and abrasion compared to the nature of the lubricant. Morin (1838) discovered that when the lubricant was continuously refreshed, the coefficient of friction was lowered by nearly half, confirming the application of the Amontons-Coulomb equation to a larger range of materials. Before the friction in lubricated bearings settles down to a lower and final steady value, Hirn (1854) determined that the test must be conducted continually for a specific time, known as the run-in period. Lubricants were often only considered to be vegetable and animal oils at the time. Petroff (1883) recognized the connection between viscosity and friction and demonstrated that a suitable selection of viscosity for each application, petroleum oils, could successfully be used as lubricants. Beauchamp Tower first discovered hydrodynamic lubrication through a series of experiments

from 1883 to 1891. Osborne Reynolds, in his classical paper of 1886, explained the load-carrying capacity of the oil film mathematically. This explanation was later expanded to address the friction issue in the more challenging case of an eccentric bearing. Lubrication research in the twentieth century was characterised by qualitative and quantitative applications of lubrication to more challenging machine elements such as screw threads, engine cylinders, gears, and cutting tools. The pursuit of a better realisation of the phenomena of imperfect lubrication and investigations of lubricant properties has led to the further development of the lubrication theory and a focus on other methods of friction reduction, such as surface engineering, solid lubrication, and superlubricity, with bearing design applications. (Luo et al., 2021; Rosenkranz et al., 2021).

2.3.1 REGIMES OF LUBRICATION

Asperities on the surfaces in contact carry the load, and the total tangential force necessary to shear these asperity junctions during sliding is typically large, resulting in excessive friction and surface damage. A lubricant is used to separate the asperities, completely or partially, to reduce frictional force and make sliding easier. The applied load is supported by the pressure created inside the lubricating fluid due to its viscous resistance to motion or by pumping the fluid lubricants between the surfaces under pressure. Regimes of lubrication are defined based on distinct situations observed with respect to the mode of lubrication arising due to an increase in load on the contacting surfaces. The regimes of lubrication specify the effectiveness of fluid film formation and hence, separation of the surface.

A thick film is maintained with the pressure produced by an external pumping agency between two surfaces having little or no relative motion under the conditions of hydrostatic lubrication. The Stribeck curve can be used to describe the lubrication regimes detected in fluid

lubrication without an external pumping source, can be given as (i) Boundary (ii) Mixed (iii) Elastohydrodynamic (EHL) and (iv) Hydrodynamic lubrication (Stribeck, 1992). The difference can be identified between hydrodynamic lubrication (thick film or perfect lubrication) and boundary lubrication (thin film or imperfect lubrication) depending on the roughness of the surfaces in any particular case (Fig. 2.2).

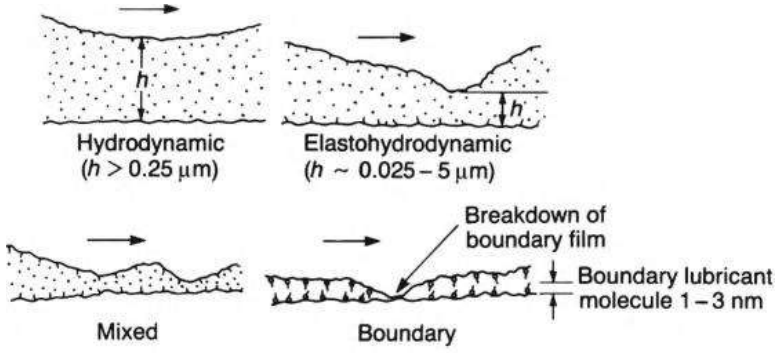

Fig. 2.2 Mean film thickness in different lubrication regimes. (Norris et al., 2008)

The term **"boundary lubrication"** refers to a situation in which the solid surfaces are close enough (typically 1–50 nm) that the load is supported by both the solid asperities and the adsorbed layer of the lubricant (Hardy, 1922). An easily sheared film on the bearing surfaces is formed by boundary lubricants, failure of which may lead to adhesive wear and chemical wear. The shear strength, hardness and melting point are the important physical properties of the contact.

Hydrodynamic lubrication occurs when the lubricant film (typically 5–500 μm) fully supports the load through viscous forces, within the space or gap between the two rubbing surfaces, solid-solid contact is prevented. In the presence of high viscosity fluids in self-acting bearings, a high load-bearing capacity can be observed at high velocities. The physical contact during start-stop operations at low surface speeds and the viscous drag cause the coefficient of friction in hydrodynamic lubrication to be as low as 0.001, and it slightly rises with sliding

speed. Adhesive wear occurs during start-stop operations in hydrodynamic lubrication, and interaction with the lubricant can cause bearing surface corrosion. (Halling, 1975)

Elastohydrodynamic lubrication (EHL) is a type of hydrodynamic lubrication in which the lubricated surfaces undergo significant elastic deformation. Elastohydrodynamic lubrication is typically linked with nonconforming surfaces or severely loaded circumstances, where high pressures can cause both lubricant viscosity changes and elastic deformation of the entities in contact. (Roberts & Tabor, 1971) EHL is divided into two types: hard EHL and soft EHL. Metals and other materials with a high elastic modulus are referred to be hard EHL. Pressure-viscosity effects and elastic deformation are both significant in this type of lubrication. The minimum film thickness is usually larger than 0.1 μm, while the maximum pressure is usually between 0.5 and 3 GPa. Rubber and other materials with a low elastic modulus are examples of soft EHL. Even with small loads, elastic distortions are substantial in soft EHL. In contrast to hard EHL, which has a maximum pressure of 1 GPa, soft EHL normally has a maximum pressure of 1 MPa and a minimum film thickness of 1 μm.

Mixed or partial lubrication occurs when elastohydrodynamically lubricated machine elements run under high pressure or low running speeds; the lubricant film created is insufficient to separate the bodies, but the hydrodynamic effects are significant. This lies in between the boundary lubrication and full film elastohydrodynamic. This lubrication regime has the majority of scientific unknowns. The molecular layers of boundary-lubricating films interact with one another. The average film thickness lies between 0.01 μm and 1 μm in a partial lubrication combination.

The transition from one regime to the other can occur with varying working conditions and be given by the Stribeck curve, which is the coefficient of friction against the bearing number ($\eta N/P$), where η is absolute viscosity, N is rotational speed in revolutions per unit second (N), and load per unit projected bearing area is P (Fig. 2.3). The lubricant film parameter

equal to h/σ (also called the lambda ratio, Λ) is sometimes used to identify the regimes of lubrication, where h, σ are mean film thickness and average standard deviation of surface heights of the two surfaces respectively. (S. Wos et al., 2015)

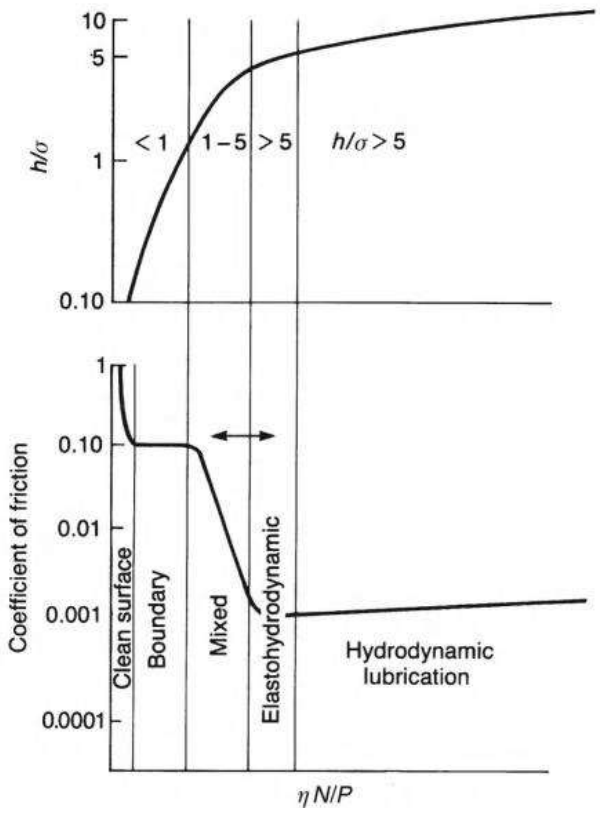

Fig. 2.3 Different regimes observed in fluid lubrication (Bhushan, 2013).

The film thickness alone cannot determine a lubrication state, as surface roughness is also required. It is convenient to use the friction coefficient to determine a lubrication state. Figure 2.4 illustrates some typical friction coefficients for the various lubrication conditions. (Wen & Huang, 2012)

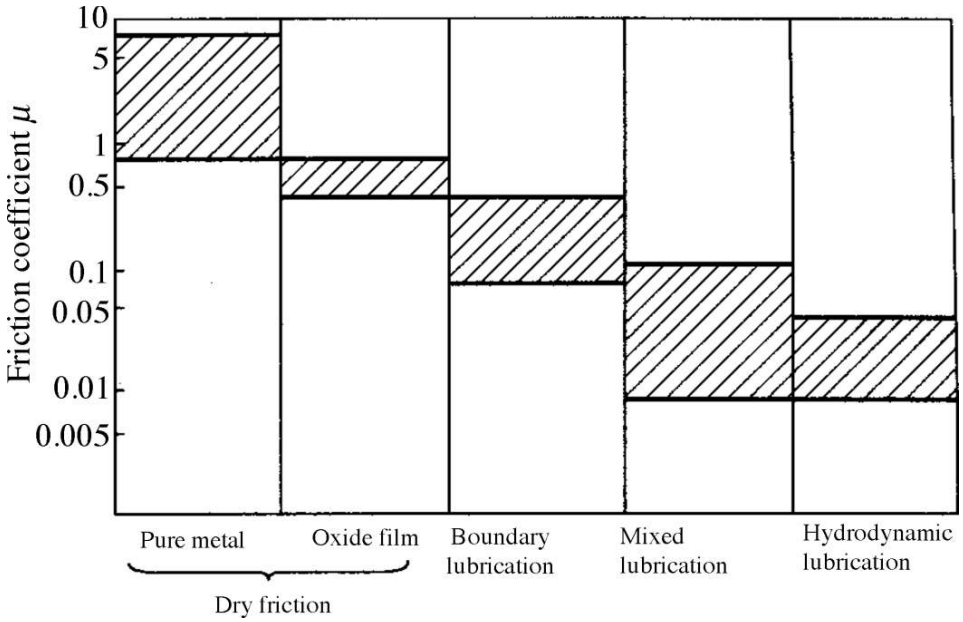

Fig. 2.4 The lubrication states and typical friction coefficients (Wen & Huang, 2012).

When the supply of lubricant is limited, investigations on starved lubrication show that friction can be reduced by surface modification. One approach to minimising friction is reducing roughness by smoothing the surfaces; however, providing an extra smooth surface is costly. As a result, surface texturing could be a reliable means of influencing the frictional behaviour of the contacts in this situation. Similar results were observed in strip drawing, where textured dies showed lower friction and produced a drawn strip with a better surface finish when compared to smooth dies. (Costa & Hutchings, 2009)

2.4 SURFACE TEXTURING

Lubrication to reduce friction and wear is a focus of tribology. However, because lubricants can be hazardous to the environment, limiting lubrication or achieving self-lubrication is preferable when only a small amount of external lubrication is required. The intricate structures with hierarchical roughness are observed in many biologically functional surfaces that define their qualities in nature. It has become possible to regulate various surface

parameters vital to making tribo-systems more environmentally friendly by surface texturing. Surface texturing has been employed for different purposes, such as controlling optical, thermal, and adsorption behaviours and improving tribological performance. (Bruzzone et al., 2008)

Surface texturing is the process of creating micro- or nanoscale cavities or projecting patches on surfaces using physical or chemical methods. Cylinder liner honing was the earliest commercial application of surface texturing (Jeng, 1996; Willis, 1986). Surface textures on these components allow for a significant reduction in friction and wear, as well as energy savings and a longer component service life. The following are widely acknowledged as potential methods for enhancing the tribological feature of surface texturing: (i) the reservoir in case of starved lubrication, (ii) the entrapment of wear debris in dry or lubricated sliding, (iii) decrease in effective contact area reducing adhesion, and (iv) the creation of micro-hydrodynamic action. (H. Zhang et al., 2016) Today, surfaces texturing is used in modern magnetic storage devices (Hausmann et al., 2009) and additionally for preventing adhesion and stiction in micro-electro-mechanical systems (MEMS) (Komvopoulos, 2003). In automotive applications, surface texture to the reciprocating surface, such as piston liners, is used for improving engine efficiency by effective means of controlling friction (Ryk et al., 2002). Hamilton et al. (1966) proposed a more analytical approach to surface texturing in the form of micro-irregularities that serve as micro-hydrodynamic bearings for parallel sliding. Etsion & Burstein (2008) demonstrated a model for mechanical seals displaying a substantial improvement in performance with regular micro-surface structure. Surface texturing of a mechanical seal minimises friction, leakage, and wear (Etsion et al., 1999). Surface texturing in bearings has been found to enhance load-carrying capacity and reduce friction (Ibatan et al., 2015). The cutting and the feed forces after texturing of cutting tools are significantly reduced, thus improving the tool life in the modern machining process (Šugár et al., 2016). Surface

texturing has recently been employed in biomedicine to tailor the biological performance of polymers now used in clinical practice. (Riveiro et al., 2018).

2.4.1 DESIGN PARAMETERS

In the event of dry sliding, the textures act as traps for wear debris, whereas the most effective tribological application of surface texturing is the improved load-bearing capacity of moving surfaces under lubricated conditions. However, establishing cost-effective surface texturing methods for the production of low-cost components and carefully designing texture patterns for surface texturing to be helpful are major challenges for the successful usage of surface texturing in tribological applications. The increase in load bearing capacity and the decrease in friction under lubricated conditions have been optimised as functions of either operational factors, such as load and speed, or texture geometric parameters, such as shape, size, and distribution of the features (Etsion et al., 1999; Ma & Zhu, 2011; Rahmani et al., 2010). Etsion and co-workers (2005) have conducted substantial research and established analytical models to solve the Reynolds equation for textured surfaces in various engineering problems. The texturing parameters are dimple shape, dimple depth, dimple density and array or distribution of dimples over the surface that compose the pattern. (Ma & Zhu, 2011; Nanbu et al., 2008; Yan et al., 2010)

2.4.1.1 DIMPLE SHAPE

The commonly used texture shapes include circular, elliptical, triangular, square and chevron. These shapes could have different depth profiles, including five shapes with a flat bottom profile; elliptical, circular, square, triangular and chevron texture shapes, and two shapes with a curved bottom profile; spherical and ellipsoidal (Fig. 2.5). (Qiu et al., 2012)

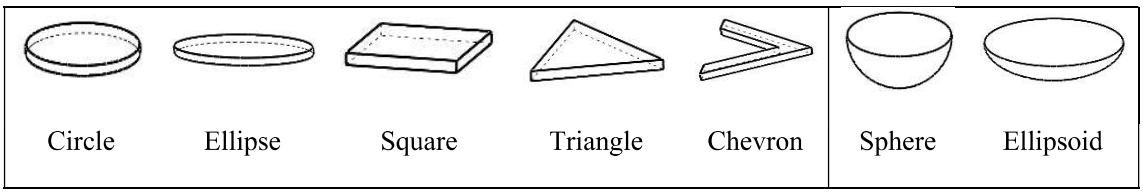

Fig. 2.5 Commonly used texture shapes with flat bottom profile (a) and curved bottom profile (b)

When compared to other shapes, a regular shape with a round or curved edge, such as an ellipse, has been demonstrated to minimise friction and increase load-carrying capacity significantly. (Shen & Khonsari, 2015). The directional dependency of textures in a triangle and trapezoidal-like shapes, such as square and rectangle is observed due to loss of symmetricity and are found to outperform regular shapes such as circle and ellipse during bidirectional hydrodynamic sliding. (Zhang et al., 2016) As shown in Fig. 2.6, the surfaces with the square texture slid in the direction indicated by arrow 2, and the triangular texture slid in the direction indicated by arrow 3 exhibit a relatively low coefficient of friction in contrast to the other orientations. These two orientations also resulted in much higher up-thrust, which reduced contact for mixed lubrication.

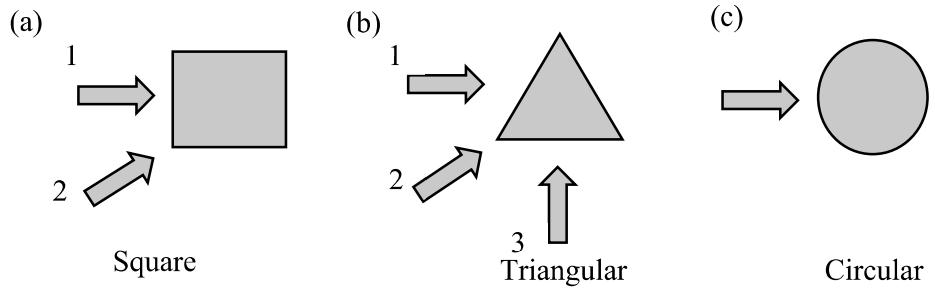

Fig. 2.6 The three types of surface texturing and six typical texture arrangements arising from directional dependency. (H. Zhang et al., 2016)

2.4.1.2 DIMPLE DEPTH

The optimum performance of textures significantly depends on the aspect ratio (ratio of depth and width) of the dimple compared to its actual geometry. Experimental works by Etsion (2005, 2006), Costa & Hutchings (2009) suggested that the size of the individual features should considerably be smaller than the contact width and the contact should be only partially textured. This limits the width of a dimple within the range of 10–100 μm. Also, a small aspect ratio, generally in the range from 0.05 to 0.15, is recommended for good results, limiting the depth of the features from around 1 to 15 μm.

Mourier et al. (2010) used numerical and experimental studies in EHL contact under rolling–sliding conditions to show that higher depth of dimples caused the oil film to collapse, but shallow dimples caused the film thickness to rise. The shear stress of the boundary layer may decrease with an increase in temperature at the contact (Briscoe et al., 1973). The lubricant's viscosity is maintained high enough when the depth is low, so shearing can expel it and increase film thickness locally.

The amount of lubricant available also affects the film thickness (Lugt & Morales, 2011). The process of replenishment of lubricant refers to the side flow, which may flow back to the contact inlet in the event of immersed contact (Guangteng et al., 1992). The starvation occurs in contact with the limited supply of the lubricant; in that case, this side flow reduces film thickness. The texture features in starved lubrication act as lubricant micro-reservoirs. However, increasing the depth or width of the dimple beyond a limit may cause a lack of benefit from textured surfaces (Ryk et al., 2002). Therefore, the aspect ratio of the cavity should be such that the load-carrying capacity to textured surfaces is achieved with a constant temperature assumption.

2.4.1.3 DIMPLE DENSITY

Etsion & Burstein (1996) suggested an optimum percentage of area density for mechanical seals with regular dimple patterns of 20%, and beyond this value, the performance rate is not much improved. The simulation results from a series of bearing models based on the Reynolds equation show that the overall hydrodynamic pressure is maximized for a range of 20–40% dimple density. (Murthy et al., 2007; Wang et al., 2003) The self-mated silicon carbide sliding in water has shown a reduction in friction for a low area density of 2.8% (Wang et al., 2001). The optimal dimple area density of 5–13% has been found preferable for friction reduction for the metallic surfaces lubricated by oil, and the area densities exceeding 20% typically result in an increase in friction. (Wang & Kato, 2003)

2.4.1.4 ARRAY OF DIMPLES

The distribution of dimples over the surface has also an effect on the tribological performance. It has been observed that in the case of cylinder liner, the presence of randomly distributed dimples caused a decrease in friction force of about 50% compared to untextured samples while tested in lubricated condition. (Grabon et al., 2013) Different arrays of dimples have been shown in fig. 2.7.

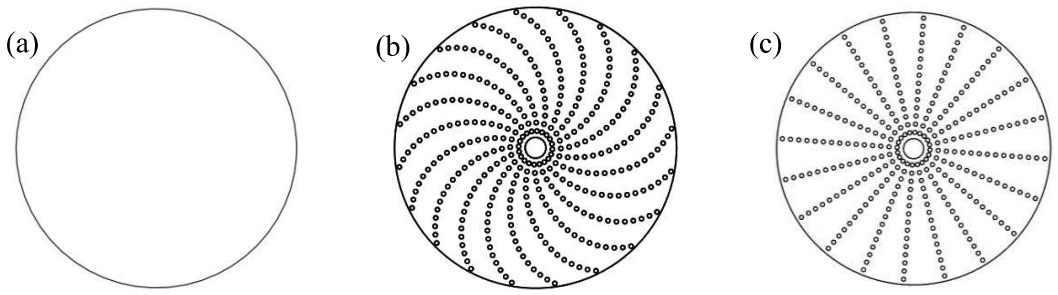

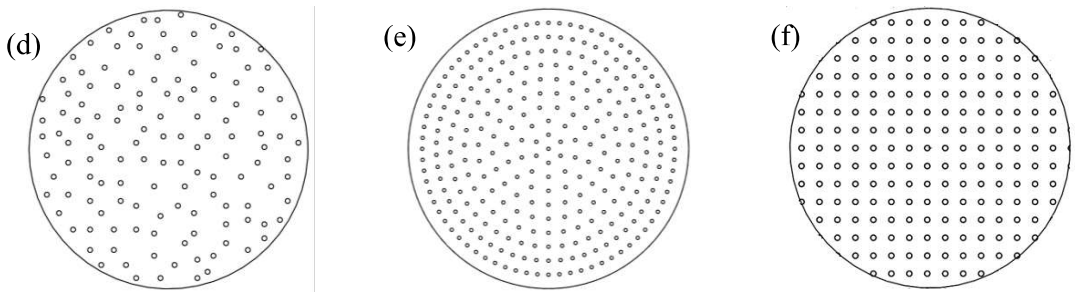

Fig. 2.7 Discs with a different array of dimples: a) untextured, b) spiral array, c) radial array, d) random array, e) concentric array, f) square array (Slawomir Wos et al., 2016)

Typically, better properties were assured by the other arrays of dimples (concentric and square) than the radial pattern. However, spiral arrays of dimples on disc surfaces had the best effect on the tribological properties of sliding parts. The friction force mean values and dispersions were lower in the spiral array of dimples than in the radial array. It's most likely due to more consistent oil pockets coming into contact with counter-specimen. (Slawomir Wos et al., 2016)

2.4.2 SURFACE TEXTURING TECHNIQUES

Various techniques of surface texturing have emerged over the years for improving tribological performance. The selection of these techniques is based on texturing speed, the simplicity of the technique, the volume of components, low cost, and flexibility in pattern geometry. The development of new engineering materials and stringent design requirements have led to the advancement of the techniques. The pattern features can be created by adding material to the chosen surface or removing material from the surface, resulting in small relief areas. The change in the surface structure can also be attributable to the redistribution of material plastically from certain parts of the surface to others.

Schneider (1984) developed the vibro-rolling method, which involves forming shallow grooves by employing a hard indenter to deform metallic parts plastically. Suh and co-workers (Saka et al., 1984) employed an etching approach to generate grooves, which was

eventually replaced by abrasive machining. Mosleh et al. (1999) termed those grooves as undulated surfaces. Electrochemical etching is a maskless process for dissolving surface material locally and leaving microsized dimples. The photolithography techniques use well-defined masks on the part surface to create the shape and layout of the features. (Pettersson & Jacobson, 2003) Reactive ion etching (RIE) is performed to remove material using high-energy chemical plasma accelerated to the part surface in a vacuum chamber. (Xiaolei Wang et al., 2003) In abrasive jet machining (AJM), the high-velocity particles are bombarded on the surface that cause the physical removal of the material. (Wakuda et al., 2003) RIE and AJM are performed using surface masking. Photolithography, electron beam, and ion beam-based texturing techniques are all high-precision techniques capable of producing nanoscale textures. Masking and remounting the pieces, as well as the necessity for advanced equipment, add to the processing time and expense of these treatments. (Gandhi et al., 2016)

Laser surface texturing (LST), out of all the viable surface patterning methods, is arguably the most sophisticated approach that combines both fast production rates and precision material removal. (Bruzzone et al., 2008; Etsion, 2005) The laser is incredibly rapid, environmentally friendly, and allows for precise control of the shape and size of micro-dimples across a wide range.

2.4.2.1 LASER SURFACE TEXTURING

Laser surface texturing (LST) uses the energy of the laser beam to create micro-features on the surface. The LST can be performed by means of laser-induced ablation (direct laser ablation), material melting by direct laser interference patterning (DLIP), and laser shock-induced surface plastic deformation for patterning(laser shock processing). (Mao et al., 2020)

2.4.2.1.1 LASER-INDUCED ABLATION

In this process, material removal occurs by irradiating a solid surface with a laser beam. The evaporation of surface materials occurs upon the absorption of laser energy due to localized heating, and the loss of the material creates a specific design pattern. (Blatter et al., 1999; Wang et al., 2001) It enables the creation of surface texture with minute features, typically with a resolution of around 1μm, and it may be used on a variety of materials such as metal, polymers, ceramics, and composites. (Semaltianos et al., 2008). This process has been used in various engineering applications such as the fabrication of micro-patterns with a diameter of around 20 μm on silicon disc (Baumgart et al., 1995), fabrication of a cone-array-like microstructure on a silicon wafer with a spike depth up to 8 μm (Wang et al., 2015), texturing of stainless steels with a dimple diameter between 200−1000 μm (Hu & Xu, 2016). An Nd-YAG laser with a pulse duration of 10 ns and a wavelength of 1064 nm was used to create textured grooves with a width of 30 μm and a depth of 12 μm on the surface of ZrO2 ceramics. (Liu et al., 2017) Laser ablation has the advantages of controllability as well as high efficiency. The technique is, however, constrained by the ejected molten material that deposits around the pockets and needs to be removed separately by polishing. This phenomenon can be regulated when very short pulses (e.g., from femtosecond lasers) are used. (Gao et al., 2011; Vincent et al., 2008)

2.4.2.1.2 DIRECT LASER INTERFERENCE PATTERNING (DLIP)

DLIP is a laser texturing technique that uses interference fields produced by several coherent high-power laser beams and allows for direct, periodically localized heating of metallic surfaces through photo-thermal interaction between laser and metal. (Zabila et al., 2009) The surface geometries, such as line, dot, and cross-like patterns, can be created in a variety of materials such as metals, polymer, ceramics and composites. DLIP has been utilized

in engineering applications such as texturing of stainless steel and 100Cr6 steel surfaces to produce one and two-dimensional periodic micropatterns. (Morales et al., 2018; Bieda et al., 2015)

The texturing speed of DLIP is substantially high with a fabrication speed of 0.1 m^2/min due to the comparable size of the interference pattern with the beam diameter, but its resolution is around 0.1 µm restricting the maximum size of the individual features too small (up to around 3 µm in width and 1 µm in depth). Therefore, such features can be too small for hydrodynamic or starved lubrication but might be desirable for EHL applications. The heating action in DLIP may also result in undesirable by-products, such as the process altering the topography of the entire surface rather than just forming localised ablated structures and thermal-induced tensile residual stresses. (Costa & Hutchings, 2015)

2.4.2.1.3 LASER SHOCK PROCESSING (LSP)

LSP is an advanced technique in which texturing is generated by a laser-induced shockwave that exceeds the yield strength of the target materials causing plastic deformation on the target surface without a thermal effect. An opaque coating covers the target material in which the laser pulse interacts instead of the target material. (Gujba & Medraj, 2014; W. Zhang & Yao, 2001)

The wear resistance of the target surface is enhanced as a result of the combined effect of compressive residual stress and the surface hardening effect caused by the laser-induced shockwave. (Yakimets et al., 2004) When compared to an untextured surface, LSP produced micro-dimple on copper showed reduced abrasive and adhesive wear (K. Li et al., 2014). Also, the wear rate of a rolled 100Cr6 steel was seen to reduce by 33 % using LSP (Yakimets et al., 2004). The application of LSP is limited to metals only.

2.4.2.2 EFFECTS OF LASER PARAMETERS ON SURFACE TEXTURING

Surface morphology and feature sizes can be modified in LST operations by adjusting laser types and processing parameters such as laser spot size, laser power intensity, and pulse repetition frequency. Lasers produce continuous light beams, also called continuous wave (CW) laser, as well as pulsed lasers, which produce powerful bursts of light of short duration (of less than a millisecond duration). The electrons absorb the energy during laser-matter interactions, which increases the kinetic energy of the system. The transfer of absorbed energy to the bulk strongly depends on the pulse duration. (Berzinš et al., 2020; Bordatchev & Nikumb, 2007; Meijer et al., 2002) For long pulse durations, laser-matter interactions are dominated by thermal conduction and diffusion as the electron and bulk subsystems have enough time to reach in thermal equilibrium leading to melting and re-solidification processes. However, because the pulse duration is too short to transmit energy to the bulk, no thermal equilibrium can be achieved between the two subsystems for ultra-short pulse durations. Direct evaporation dominates the laser-matter interaction, but a mixture of melting and re-solidification, as well as direct evaporation, can be found. (Leitz et al., 2011) The laser pulse duration, which impacts the heat input in laser ablation and interference, as well as the plastic deformation, has a substantial impact on the process efficiency and effectiveness of laser surface texturing.

The commercial pulse lasers used for surface texturing are milli-second (ms), nano-second (ns), pico-second (ps), and femto-second (fs) lasers based on laser pulse duration. Figure 2.8 (a-d) shows the schematics of laser processing with steel as the target material. The fs and ps lasers show surface ablation and no hardening effect due to very short pulse duration (Fig. 2.8 (a)). The ns laser produced more heat than ultrashort pulses, resulting in the removal of surface material as well as the hardness of the surrounding area (Fig. 2.8 (b)). The interaction

of ms laser produced a hardened surface with a tempered zone of intermediate hardness in the target material (Fig. 12(c)). The CW laser beam hardening led to a larger heat-affected zone due to the longer interaction of beams with the target material (Fig. 2.8 (d)). The absence of a distinct tempered zone as in case of ms laser suggests that the heat dissipating into bulk of the material is more uniform. (Maharjan et al., 2019; Mao et al., 2020) Because of the smaller heat affected zone, ultra-short pulse lasers (ps/fs) can fabricate higher-quality surface features. The processing time is also lowered; nevertheless, from a practical standpoint, the higher cost of the equipment is a major worry.

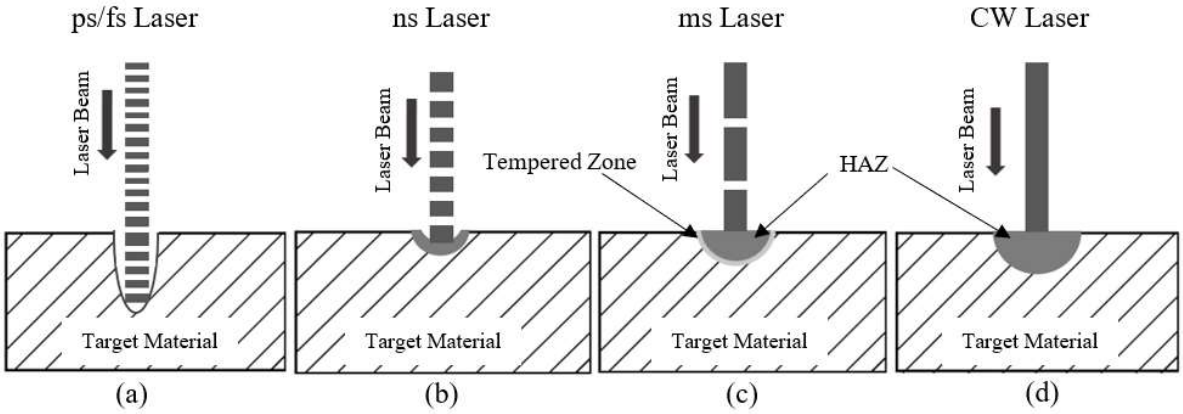

Fig. 2.8 Schematics of laser processing using–(a) fs and ps laser (b) ns laser (c) ms; and (d) cw laser. (Maharjan et al., 2019)

The laser power intensity and number of pulses also have an effect on depth and width of the dimple. The depth and width of dimples on the surface of 314 stainless steels considerably increased with an increase in laser pulse energy during laser ablation. (Dunn et al., 2014) Similarly, the depth and diameter of the dimple on 100Cr6 steel surface fabricated by laser ablation, increased with the increase of the number of pulses. (Grabowski et al., 2018) The power of a short-pulsed laser can be increased enormous by Q-switching. This technique is mainly applied to nanosecond pulses for obtaining high-energy pulses from a laser by modulating the intracavity losses and, thus the Q factor of the laser resonator. The Q

factor (quality factor) of a resonator is a measure of the strength of the damping of its oscillations.

The pulsed Nd:YAG lasers are readily suitable for applications that require narrow kerf widths, small heat-affected zones (HAZ) and difficult-to-cut profiles. Nd:YAG lasers emit a high-intensity light with a wavelength of 1064 nm in the infrared region of the electromagnetic spectrum. It has high absorption rate due to its shorter wavelength, which enables to process highly reflective materials using relatively less laser power. Nd:YAG lasers, also due to its economic advantage, are used to process a wide variety of materials such as carbon steels, nickel and aluminium-base alloys, fibre reinforced panels, graphite epoxy composites, etc. (Etsion, 2005; Thawari et al., 2005)

2.5 FRICTION AND WEAR TESTING

Various factors, including the materials, topographical features, and geometrical characteristics of surfaces in mechanical contact and sliding against each other, influence friction and wear between them. The test specimens (or tribo-elements), and the test conditions, along with some supporting auxiliary subsystems, form a tribosystem for studying behaviours on or between the interacting surfaces in relative motion (Fig. 2.9) (Xie, 1996). The results obtained from friction and wear analysis by conducting a tribotest are used to understand underlying fundamental mechanisms, determine the life of a rubbing component, select or develop materials, variables for new applications, etc. The five main areas pivotal to tribotesting include the material parameters, operational parameters such as contact geometry, loading, motion and the environmental parameters in which a tribosystem operates.

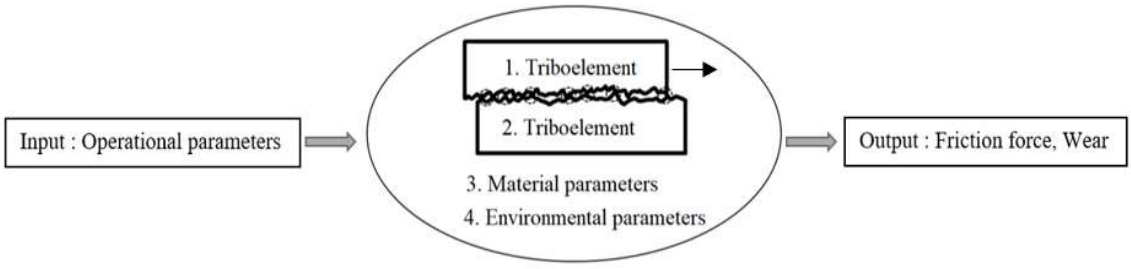

Fig. 2.9 The various components constituting a tribosystem.

The surface may have oxides, coatings, adsorbed layers and contaminants, as well as properties of bulk material with basic composition and the processing history, which need to be considered. When in friction with loading, the ductile metals can be characterized by the appearance of seizure (Semenov, 1980). The metals are alloyed to obtain high wear resistance. The polymers, with their ability to provide reasonably low friction coefficients and wear, are used in unlubricated conditions or as solid lubricant materials compared to metallic and ceramic surfaces. The nano-coatings are applied to produce low-wear metal-on-metal contacts, particularly in dry condition. (Sawyer et al., 2014) It has been observed that an increase in materials hardness shows better wear resistance and a lower value of contact friction (Jain et al., 2021). Metals with high hardness, and a low tendency for plastic deformation, such as nickel and chromium, exhibit relatively low coefficients of friction (Mokhtar, 1982). The geometry of the contacting surfaces affects friction and wear. Michalczewski et al. (2000) conducted experiments on four different contact pairs having identical test parameters, both for conformal and non-conformal friction contacts, and the results were different. The load and the sliding speed affect wear and the amount of friction force. The applied load affects the frictional force as the contact area increases and causes deformation as the friction arises on the peak points of the asperities. The friction coefficient is not affected by the applied load in case of plastic deformation. The coefficient of friction doesn't depend on the sliding velocity if the nature of surface layer to doesn't change. However, the sliding velocity leads to an increase in the temperature, resulting in softening of metal, change in the coefficient of friction and wear

(Halling, 1975). Hsu et al. (2014) in their patent, mentions operating regime classification and mechanisms. Regime (I) infers high speed (1 m/s), low load (15 MPa) and majorly have hydrodynamic effects and demonstrated success in seals, thrust bearings. The regime (II), which has a high to medium speed and a medium load, produces a combination of hydrodynamic and contact mechanic effects, which increases friction. At low-medium speed, high load, the combined effects of contact mechanics, lubricant compressibility, and wear particle trapping are exhibited (III). The operating environment of a tribosystem has an impact on its performance. Dry friction is substantially higher in regular engineering materials, and lubricants are utilised to reduce the overall friction coefficient by separating the surfaces and creating a lubrication layer. Unlike dry friction, lubricated friction is affected by operational variables, including sliding speed, lubricant viscosity, temperature, and so on. The lubricant viscosity reduces when the speed is low, the load is high or the temperature is sufficiently large (Wang & Wang, 2013).

The tribological test methods are adopted according to their realism degree. The tribo-surfaces in contact are replaced by simulated components while conducting the laboratory model tests considering the test time, cost, and the accurate control of test conditions (Gahr, 1987). In sliding contact, wear based on adhesion or abrasion are most common (Antler, 1981). The model tests are performed most commonly on asymmetrical pin-on-disc rigs for sliding wear tests due to their simplicity and versatility in test conditions and specimen shape. (Fig. 2.10).

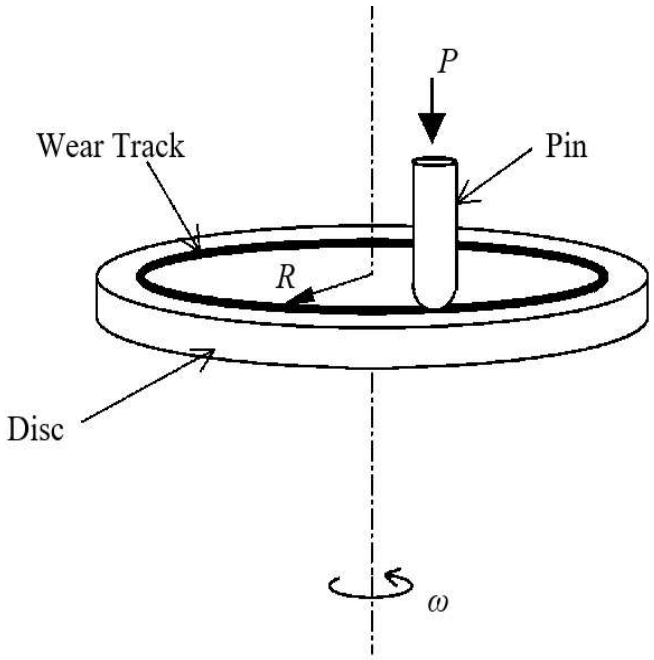

Fig. 2.10. Schematic illustration of a pin-on-disc wear test

2.6 FRICTION AND WEAR OF TEXTURED STEELS

The frictional and wear behaviour of textured surfaces under dry, lubricated conditions have been experimentally studied. The impact of texture has a comprehensive result of the positive role of enhancing the tribological performance.

2.6.1 DRY CONDITION

The laser textured stainless steel surface and the balls made of 100Cr6 steel with periodic line pattern were tested under dry sliding conditions for two relative alignments of the line pattern ($0^o/90^o$) (Gachot et al., 2013). The polished reference surface exhibited a larger coefficient of friction value than the textured specimens, irrespective of the relative alignment (0°/90°) between the sliding surfaces. However, in the case of laser-patterned surfaces, the coefficient of friction reduced for 90° orientation due to less relative contact area as compared with 0° orientation, however, it was independent on the periodicity of the pattern. The wear

was more in the case of 0° alignment, as compared to 90° orientation due difference in interlocking of induced patterns. The results demonstrated that surface texturing reduces the real area of contact under dry conditions, lowering the frictional force and, consequently the coefficient of friction (Fig. 2.11 (a)).

In a similar experiment, the wear particles in the contact zone depicted continuous agglomeration and collapse under dry conditions, resulting in a much-varied coefficient of friction value. The textured surfaces act as storage volumes for the worn particles, reducing abrasion and lowering friction (Fig. 2.11(b)). (Hwang et al., 1999; Rosenkranz et al., 2014) However, the stress concentrations in the contacting spots are observed to increase due to the reduced actual contact area of textured surfaces under dry friction and in non-conformal contacts, which may further lead to an increased wear rate (Ripoll et al., 2011). The bulges present around dimples are hard deposits which may increase the wear and change the coefficient of friction (Jian Li & Wang, 2013). The pin-on-disc wear test of nitriding steel slid against a pin of 100Cr6 steel shows the evolution of the coefficient of friction for the untextured and textured surfaces under the dry condition at a normal load of 1 N and sliding speeds ranging from 1 to 12 cm/s. The coefficient of friction for the untextured surface was observed to rise quickly up to 1.0 and stabilize, whereas it increases more slowly in the case of textured surface. Both textured and untextured couplings experience seizure when the typical load is increased to 3 N (Borghi et al., 2008). On the other hand, the surface with higher dimples density having high volumes can capture more wear debris, leading to reduced wear and resulting in the lowest and steady friction coefficients (Segu & Hwang, 2015).

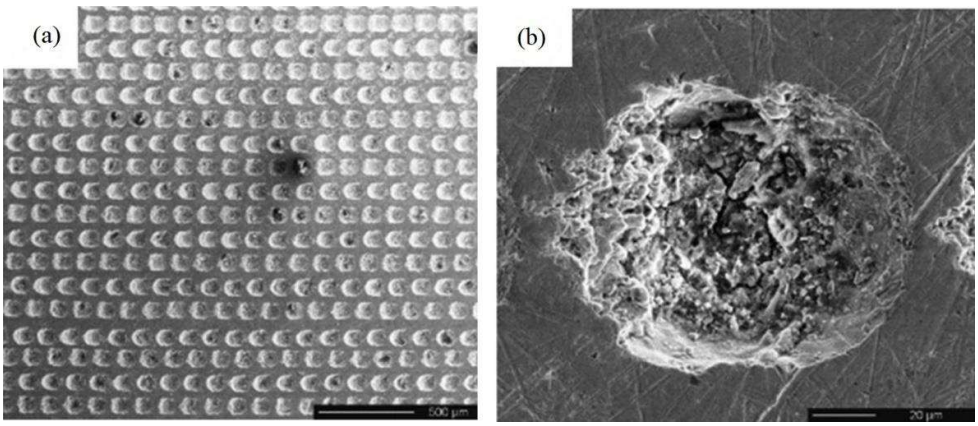

Fig. 2.11 SEM images of laser textured 30 NiCrMo12 nitride steel (a); an individual dimple filled with the wear debris (b) (Mao et al., 2020)

The ploughing action of the asperities causes the transfer of material which may lead to a transfer layer formation due to the adhesion component of friction. Menezes et al. (2006) observed during the sliding of an aluminium pin over EN8 flats that surfaces with random texture had increased adhesion component but were constant for the other surfaces. In addition, as the typical load increases, the amount of the transfer layer increases.

The conventional and well-established Archard's law of wear (Archard, 1953), is used to calculate the sliding wear ‘w’ through the relation (Bhushan, 2013):

$$w = k\frac{Pl}{H}$$

Where k is a nondimensional wear coefficient, P is applied load, l is sliding distance, and H is the hardness of the softer material. The wear coefficient k depends on the material system and needs to be calculated experimentally.

2.6.2 LUBRICATED CONDITION

The laser textured surface produces a high number of micro-dimples (Fig. 2.11(a)), which can produce a micro-hydrodynamic effect in full or mixed lubrication or a micro-

reservoir for lubricant under limited supply of lubrication situations. When the lubricant is introduced between two parallel surfaces moving at the same relative sliding velocity, viscous shear occurs exclusively, with no influence on the pressure between the two flat surfaces, resulting in zero load (F) carrying capacity (Fig. 2.12 (a)). The velocity distribution between the converging surfaces of finite length is shown in the Fig. 2.12 (b). Since the cross-section area at the inlet is more than the outlet, to maintain the continuity of the fluid into a converging region creates a lift pressure between the surfaces. In a similar situation, the presence of a micro-texture causes a hydrodynamic pressure distribution by changing the local film thickness into a converging-diverging one. (Tang et al., 2013)

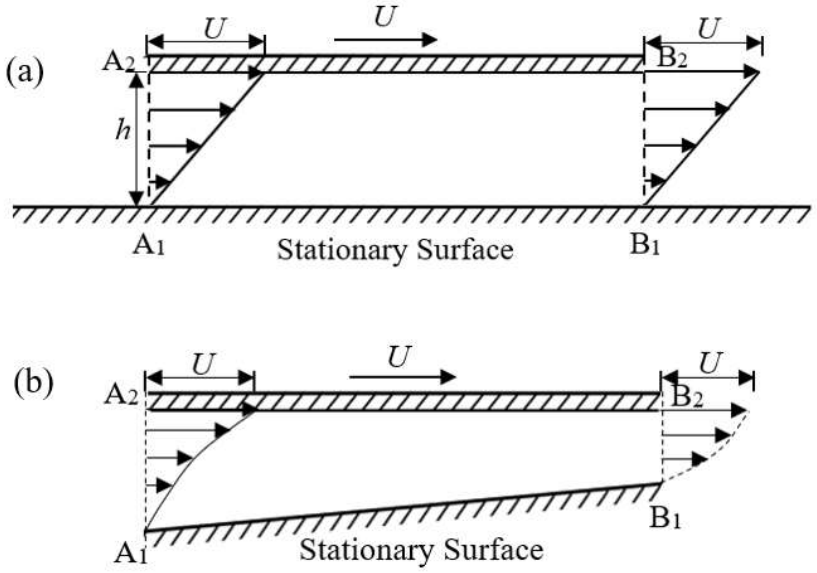

Fig. 2.12 Mechanism of pressure development: velocity distribution – parallel surfaces (a); velocity distribution – non – parallel surfaces (b).

Figure 2.13 shows a schematic illustration of two parallel surfaces. The lower surface having a single dimple is moving at sliding velocity U relative to the upper surface (Fig. 2.13(a)). P_a is the ambient pressure surrounding the two surfaces, F is the load carrying capacity, P_c is the cavitation pressure. The pressure distribution due to the presence of a micro-

cavity is shown in Fig. 2.13 (b). The pressure in the diverging portion decreases below P_a and increases above P_a in the converging portion of the dimple. The pressure distributions at a lower velocity are anti-symmetric about P_a due to a smaller maximum pressure than the net value of the cavitation pressure P_c. This distribution gives a zero net pressure distribution along the horizontal axis resulting in zero load carrying capacity. Because the minimum pressure value is constrained below by the cavitation pressure, increasing the velocity raises the maximum pressure in the region, and the pressure distribution becomes asymmetric about P_a. Overall pressure has a net positive value. (Etsion, 2013; Hamilton et al., 1966)

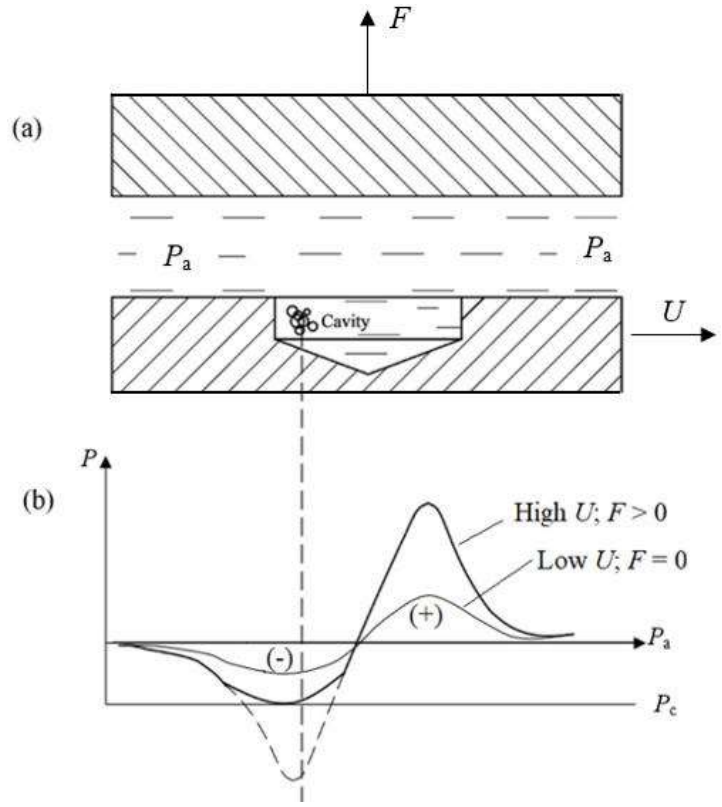

Fig. 2.13 Schematic illustration of parallel sliding surfaces with a single dimple (a), and the distribution of hydrodynamic pressure over the single dimple (b) (Tang et al., 2013)

The individual dimples from the sum of their collective contributions increase the total load-carrying capacity of the textured surface. Figure 2.14 (a) illustrates a partial laser surface

textured parallel slider bearing cross-section, and (b) shows the load carrying capacity as a function of texture distribution parameters. Conformal mating surfaces will be more advantageous in obtaining the total load-carrying capacity of textured parallel surfaces due to the micro-scale feature of the dimples. Also, the dimples, rather than the asperities, are a better choice due to having a larger real contact area, and easy manufacturing. (Etsion, 2013)

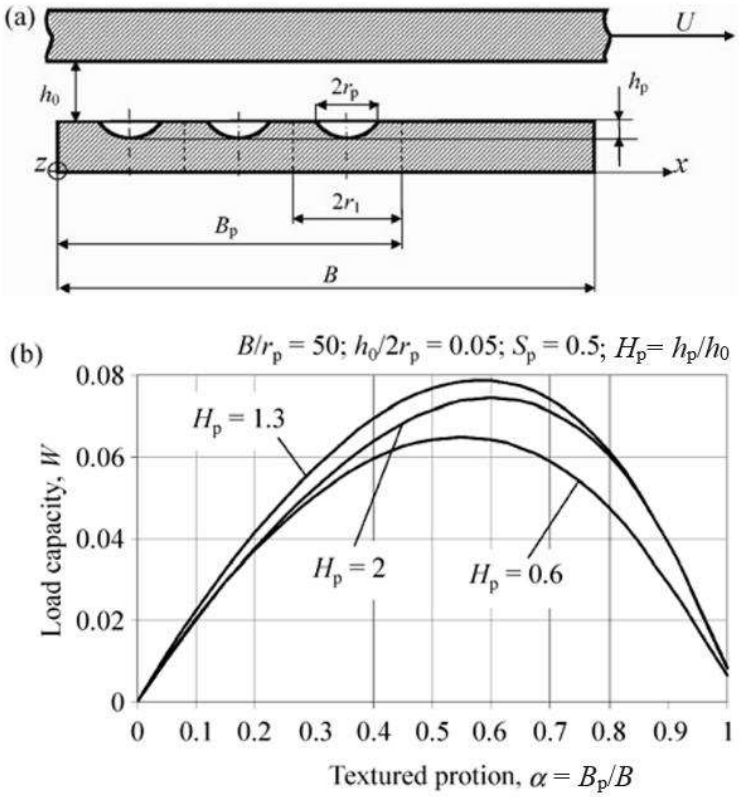

Fig. 2.14 (a) A partial laser surface textured parallel slider bearing cross-section. (b) The effect of the texturing on the load-bearing capacity. (Etsion, 2013)

Galda et al. (2009) observed that the distribution of oil pockets and their shape primarily affect the lubrication regime transitions. Kovalchenko et al. (2017) found that in conformal contact, the hydrodynamic effect was more noticeable at higher loads, speeds and with higher viscosity oil, and extended the low-friction full hydrodynamic regime to mixed and boundary lubrication regimes at higher loads and slower speeds as well. At the lowest sliding speed, the discs having

higher dimple density showed the highest friction coefficient, and a lower texture density showed the best results. The extent of surface damage and wear under a hydrodynamic lubrication regime is likely to be small compared to surfaces operating under boundary lubrication. Tang et al. (2013) concluded that a 5% density could reduce friction up to 38% and wear up to 72%. In a similar study, a surface with 12% texture density in flat-on-flat tribotest (Segu & Hwang, 2015), showed a reduction in the average friction coefficients when sliding speed was increased from 0.09 m/s to 0.18 m/s and maintained a low value for a speed up to 0.55 m/s. As the sliding speed increased, more fluid entered the contact surface, so hydrodynamic lubrication may have played a significant role in lowering friction in this case.

Ryk et al. (2002) found that in a limited supply, the dimples act as storage of the lubricant, which also affects the film thickness, and the texturing is beneficial for optimal dimple depth and low lubricant viscosity across the entire range of measured flow rates. Surface texturing, on the other hand, may not be very useful in the presence of high viscosity lubricant or the deepest dimples under particular operating conditions. The textures with smaller grooves and perpendicular orientation across the sliding direction had significantly lower friction and wear resistance than the untextured surface. (Pettersson & Jacobson, 2004).

2.7 FORMULATION OF THE PROBLEM

From the above review of the available literature, one may infer that despite a lot of work done on the analysis of LST on friction and wear performance, there is still a scope of exploration about the characteristic of dimples and tribological behaviour under various conditions. Most of the tribological studies have been carried out with the single standard shape of the dimples under low speed, low load, or high load. To the best of our knowledge, investigations on the tribological performance of new texture shapes like Bi-triangular (BT) having different densities under dry sliding as well as a limited supply of the lubricant have not

been reported so far. This is the major research gap and worked as the prime motivation to carry out the present study.

Therefore, the current study is motivated by a need to unravel the effect of texture geometry, its array, and density on friction and wear behaviour bearing steel which are used in various applications under different loads and speeds under dry as well as lubricating conditions with a limited supply of lubricant using conformal contact geometry under unidirectional sliding

In essence, the present study has been carried out with the following objectives.

i. To texture the surface having different shape, densities and array of dimples.
ii. To explore the friction and wear behavior of the laser textured surfaces at different loads and speeds under dry sliding.
iii. To find the optimal density and shape of the texture in dry sliding conditions.
iv. To evaluate the tribological performance of the laser textured surface at different loads and speeds under limited supply of lubricant.
v. To establish the dominant mechanisms of wear.